

Properties of Localization Using Distance-Differences

Xiaochun Xu and Sartaj Sahni

Computer and Information Science and Engineering Department

University of Florida

Gainesville, FL 32611

Email: {xxu,sahni}@cise.ufl.edu

Nageswara S. V. Rao

Computer Science and Mathematics Division

Oak Ridge National Laboratory

Oak Ridge, TN 37831

Email: raons@ornl.gov

Abstract— We study several basic properties related to the task of localizing a source using distance-difference measurements to it. These properties enable minimalistic realizations of localization systems. We establish conditions for the unique identification of a source in Euclidean plane, and derive minimum number of sensors needed for unique source identification within the Euclidean plane and a polygonal monitoring region. Compared to four possible intersections of two hyperbolas, this task leads to at most 2 intersections, which correspond to potential source estimates.

I. INTRODUCTION

The Difference of Time-of-Arrival (DTOA) localization problem deals with estimating the location of a source using distance-difference measurements from multiple sensors. This classical problem has been extensively studied in applications in aerospace systems [1], [2], wireless communication networks [3], and wireless sensor networks [4], [5]. There are two basic formulations of the DTOA localization problem: (i) the distance-differences to a source are measured from known sensor locations, and the problem is to estimate the location of the source; and (ii) a device (i.e., a mobile node) receives distance-differences from beacon nodes with known locations, and the problem is to estimate the location of the device, that is self-localization. The classic DTOA localization methods include two general approaches: (i) linear algebraic solution which typically involves matrix inversion and solution to a quadratic equation [6], [7], [2], and (ii) application of general intersection method of hyperbolic curves [8].

The renewed interest in this problem is in part due to the need for minimalistic implementations suitable for nodes with limited computational resources and networks with limited number of sensors. In terms of computation, the computational geometry method for DTOA localization in Euclidean plane [10], [11], [12] offers efficient computation. This method employs a binary search on a distance-difference curve in R^2 using a second distance-difference as the objective function. To support the binary search, this method establishes the unimodality of the directional derivative of the objective function

within each of a small number of suitably decomposed regions of R^2 [12]. However, despite the extensive literature on DTOA localization, several basic aspects needed for minimalistic network realizations do not seem to be reported.

In this paper, we present a number of results that establish basic properties of DTOA localization. We first consider the unique identification of a source and establish the following:

- 1) DTOA localization uniquely identifies a source in Euclidean plane R^2 iff the sensors do not lie on a hyperbola¹.
- 2) At least four sensors are necessary for unique localization of a source in Euclidean plane, and it is sufficient to place the four sensors at the corners of a parallelogram to achieve this.
- 3) A minimal sensor set to achieve unique source identification (i.e., a sensor set none of whose proper subsets is also a uniquely identifying sensor set) has between 4 and 6 sensors.
- 4) Three sensors are sufficient to uniquely identify any source in a monitoring region bounded by a polygon. These sensors, however, must be placed outside the polygon.

We then consider the computational aspects of DTOA localization that utilizes the intersection of hyperbolas corresponding to distance-difference measurements. In general, two hyperbolas may have four intersection points, but we show that two hyperbolas that correspond to distance-differences to a source that have a common focus may have at most 2 intersections. We also show that when non-collinear sensors are used, at most 2 points can have the same DTOA values. These results establish that the DTOA problem is more structured and easier in this sense compared to computing intersection points of hyperbolas.

This paper is organized as follows. In Section II, we present some fundamental properties and definitions. Properties of

¹For convenience, in this paper, the term hyperbola is used to refer to even a portion of a hyperbola.

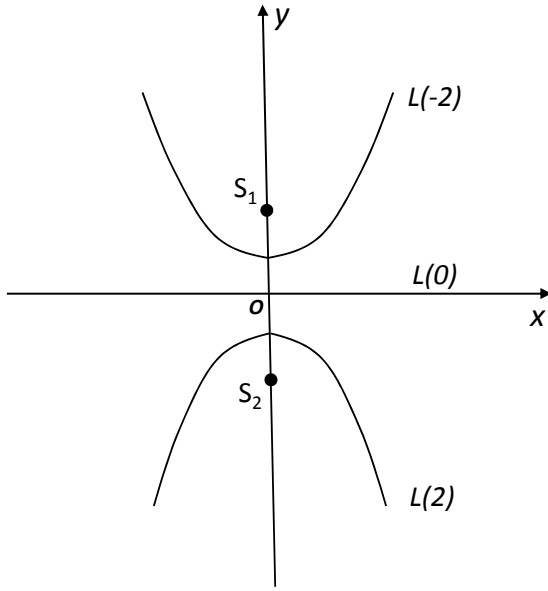


Fig. 1. Examples of the locus L_{12}

sensor sets that uniquely identify all sources in Euclidean space are developed in Section III. Our detailed analysis of Section IV establishes the bound on the the number of intersections of two DTOA hyperbolas. In Section V we show that at most 2 points can have the same set of DTOA values. The minimum number of sensors needed to uniquely identify all sources in a bounding polygon is derived in Section VI. Finally, we conclude in Section VII.

II. PRELIMINARIES AND DEFINITIONS

Let $S_i = (x_i, y_i)$, $1 \leq i \leq k$, be the locations of k sensors in Euclidean space R^2 . These locations are assumed to be distinct. For any point $P = (x, y)$ in R^2 , the distance, $d(P, S_i)$, between P and S_i is $\sqrt{(x-x_i)^2 + (y-y_i)^2}$. A signal originating at P at time 0 arrives at S_i at time proportional to $d(P, S_i)$. For simplicity, we assume that the arrival time is $d(P, S_i)$. The difference, Δ_{ij} , in the time of arrival (DTOA) at S_i and S_j is given by

$$\Delta_{ij}(P) = d(P, S_i) - d(P, S_j).$$

From the triangle inequality, it follows that $|\Delta_{ij}(P)| \leq d(S_i, S_j)$. Furthermore, the locus, $L_{ij}(\delta)$, of points defined by

$$L_{ij}(\delta) = \{P | \Delta_{ij}(P) = \delta\}$$

is a hyperbola² (see Figure 1).

In this paper, we consider the *DTOA localization* problem of estimating the location of a source S from the measurements of $\Delta_{ij}(S)$, $1 \leq i < j \leq k$. When $\Delta_{ij}(P) = \Delta_{ij}(Q)$ for every $i, j \in \{1, 2, \dots, k\}$, the points P and Q are indistinguishable. Actually, since $\Delta_{ij}(P) = \Delta_{1j}(P) - \Delta_{1i}(P)$, for all i and j , P and Q are indistinguishable iff $\Delta_{1j}(P) = \Delta_{1j}(Q)$ for every $j \in \{2, \dots, k\}$. So, the set of sensor locations (also referred to as the sensor set) $SS = \{S_1, S_2, \dots, S_k\}$ can uniquely identify

²Strictly speaking, $L_{ij}(\delta)$ is one branch of a hyperbola and $L_{ij}(-\delta)$ is the other branch. As mentioned earlier, for convenience, in this paper, we use the term hyperbola to refer to one branch of a hyperbola.

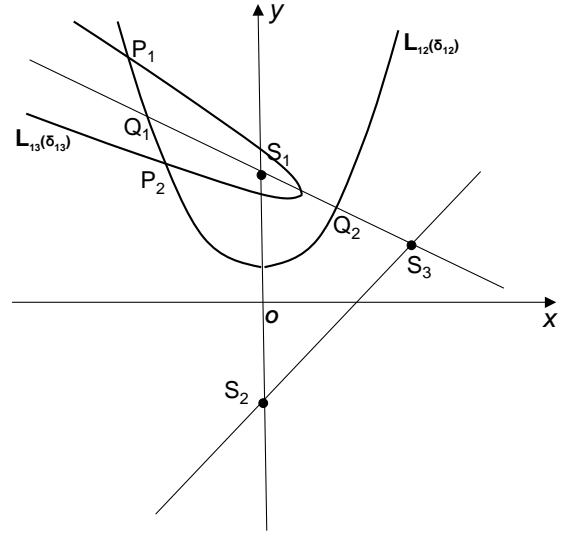


Fig. 2. Three non-collinear sensors S_1 , S_2 , and S_3 form a triangle and two hyperbolas $L_{12}(\delta_{12})$ and $L_{13}(\delta_{13})$ intersect each other at P_1 and P_2 .

every source S in Euclidean space R^2 iff for every pair P and Q of distinct points in Euclidean space R^2 , we have $\Delta_{1j}(P) \neq \Delta_{1j}(Q)$ for at least one $j \in \{2, 3, \dots, k\}$. A sensor set that can uniquely identify (localize) every possible point in Euclidean space is called an *identifying sensor set*, *ISS*. Two points that are indistinguishable are *duals*.

The DTOA method localizes the source by determining the common intersections of the hyperbolas³ $L_{1j}(\Delta_{1j}(S))$, $2 \leq j \leq k$. When these hyperbolas have more than one common intersection, the source is not uniquely localized. Figure 2 gives an example of two hyperbolas $L_{12}(\delta_{12})$ and $L_{13}(\delta_{13})$ that intersect at two distinct locations P_1 and P_2 . So, using L_{12} and L_{13} alone, we are unable to uniquely localize the source. We are able only to assert that the source location is either P_1 or P_2 . To uniquely identify the source using the DTOA method, the hyperbolas L_{1j} , $2 \leq j \leq k$ should have exactly one common intersection. Alternatively, these hyperbolas should have exactly one common intersection inside a region in which the source is known to lie.

III. PROPERTIES OF IDENTIFYING SENSOR SETS

In this section, we establish, in Theorem 1 a necessary and sufficient condition for a sensor set SS to be an *ISS*. Theorem 2 shows that every *ISS* has at least 4 sensors and Theorem 4 shows that every *ISS* with more than 6 sensors has a subset of size at most 6 that is an *ISS*.

Theorem 1: The sensor set $SS = \{S_1, \dots, S_k\}$ is an *ISS* iff no hyperbola passes through all points of SS .

Proof:

We first show that if SS is an *ISS*, then no hyperbola may pass through all points of SS . By contradiction, suppose there exists a hyperbola, say L , that passes through all points of in SS . Let P_1 and P_2 be the two foci of L . From the definition of a hyperbola, it follows that $d(P_1, S_i) - d(P_2, S_i) = d(P_1, S_j) - d(P_2, S_j)$, $1 \leq i < j \leq k$. So, $\Delta_{ij}(P_1) = d(P_1, S_i) - d(P_1, S_j) =$

³A point in R^2 is a common intersection of a set of hyperbolas iff this point is on each of the hyperbolas

$d(P_2, S_i) - d(P_2, S_j) = \Delta_{ij}(P_2)$, $1 \leq i < j \leq k$. Hence, P_1 and P_2 are indistinguishable and SS is not an *ISS*, a contradiction.

Next, we show that if SS is not an *ISS*, then at least one hyperbola passes through all points of SS . Let P_1 and P_2 be two different points that are indistinguishable. So, $\Delta_{1j}(P_1) = d(P_1, S_1) - d(P_1, S_j) = d(P_2, S_1) - d(P_2, S_j) = \Delta_{1j}(P_2)$, $2 \leq j \leq k$. Hence, $d(P_1, S_1) - d(P_2, S_1) = d(P_1, S_j) - d(P_2, S_j)$, $2 \leq j \leq k$. Therefore there is a hyperbola with P_1 and P_2 as its foci that passes through all points of SS . ■

Theorem 2: If SS is an *ISS*, then $|SS| \geq 4$ and there exist *ISS*s that have exactly 4 sensors.

Proof:

We first prove that 3 sensors are not sufficient to constitute an *ISS* and so, $|SS| \geq 4$ whenever SS is an *ISS*. Let $SS = \{S_1, S_2, S_3\}$. When S_1, S_2 , and S_3 are collinear, the straight line through these three sensors is a trivial hyperbola through the points of SS . From Theorem 1, it follows that SS is not an *ISS*. When S_1, S_2 , and S_3 are not collinear, they define a nontrivial triangle as shown in Figure 2. Clearly, there exists a negative constant, δ_{12} , such that the hyperbola $L_{12}(\delta_{12})$ intersects the line S_1S_3 at two distinct points Q_1 and Q_2 . Observe that the hyperbola $L_{13}(-d(S_1, S_3))$ is actually a ray that originates at S_1 and intersects $L_{12}(\delta_{12})$ at Q_1 only. Let δ_{13} be a negative constant slightly greater than $-d(S_1, S_3)$. The hyperbola $L_{13}(\delta_{13})$ intersects $L_{12}(\delta_{12})$ at two distinct points P_1 and P_2 (see Figure 2). So, P_1 and P_2 are indistinguishable and SS is not an *ISS*.

Next, we show that whenever $SS = \{S_1, S_2, S_3, S_4\}$ are the corners of a parallelogram with side length > 0 , SS is an *ISS*. We show this by proving that no 4 distinct points of a hyperbola define the corners of a parallelogram. The result then follows from Theorem 1.

Consider the hyperbola L of Figure 3. Let S_1, S_2, S_3 , and S_4 be 4 points on this hyperbola. The case shown in Figure 3 has S_1 and S_4 on one part (arm) of the hyperbola and S_2 and S_3 on the second part. (There are two other cases for the location of the 4 points—exactly 3 points on one part of L and 4 points on one part of L .) Let Q_1 and Q_2 , respectively, be the intersections of the line segments $\overline{S_1S_2}$ and $\overline{S_3S_4}$ with the x -axis, which is the semimajor axis of L . If the 4 identified points on L are the corners of a parallelogram, $\overline{S_1S_2}$ and $\overline{S_3S_4}$ are parallel and of equal length. However, if these segments are parallel, $d(S_1, Q_1) < d(S_4, Q_2)$ and $d(S_2, Q_1) < d(S_3, Q_2)$. So, $d(S_1, S_2) = d(S_1, Q_1) + d(S_2, Q_1) < d(S_4, Q_2) + d(S_3, Q_2) = d(S_3, S_4)$. So, $\overline{S_1S_2}$ and $\overline{S_3S_4}$ cannot be parallel and of equal length. The remaining two cases are similar. ■

Corollary 1: An infinite number of hyperbolas pass through any 3 non-collinear sensors in Euclidean space R^2 .

Corollary 2: Whenever SS contains the corners of a parallelogram with side length > 0 , SS is an *ISS*. In particular, whenever 4 sensors of SS are at the 4 corners of a square with side length > 0 , SS is an *ISS*.

An *ISS* is a *minimal ISS (MISS)* iff no proper subset of the *ISS* is also an *ISS*. Theorem 4 establishes an upper bound of 6 on the size of an *MISS*. To prove this theorem, we need to use Bezout's bound on the number of intersections of curves in Euclidean space.

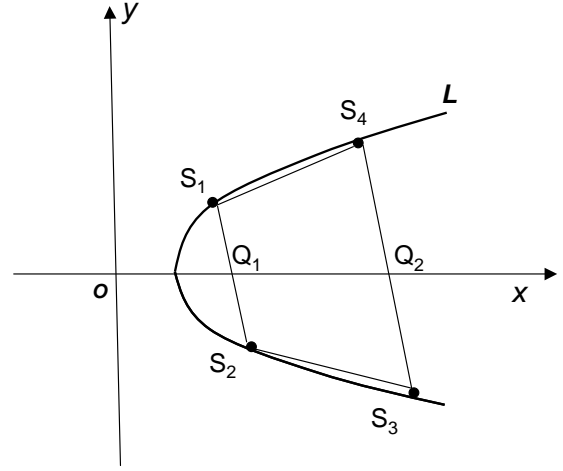


Fig. 3. A hyperbola L that passes through S_i ($1 \leq i \leq 4$).

Theorem 3: [Bezout's Theorem [13]]: Let C_1 and C_2 be curves of degree m and n , respectively, in Euclidean space R^2 . If C_1 and C_2 have no curves in common, then the number of intersections of C_1 and C_2 is at most mn .

Corollary 3: Two hyperbolas in Euclidean space R^2 have at most 4 intersections.

Lemma 1: At most 1 hyperbola may pass through any set of 5 or more distinct points.

Proof: Consider any set SS with 5 or more points. If two hyperbolas pass through the points of SS , then these two hyperbolas intersect at the points of SS and so have more than 4 intersections. This violates Corollary 3. Hence, at most 1 hyperbola may pass through the points of SS . ■

Theorem 4: Every SS that is a *MISS* satisfies $4 \leq |SS| \leq 6$.

Proof: $4 \leq |SS|$ follows from Theorem 2 and the fact that a *MISS* is an *ISS*. $|SS| \leq 6$ may be shown by contradiction. Suppose that $|SS| > 6$. Let SS' be a subset of SS such that $|SS'| = 5$. From Lemma 1, SS' has at most 1 hyperbola passing through its 5 points. If no hyperbola passes through these points, then SS' is an *ISS* (Theorem 1) and SS cannot be an *MISS*. So, we may assume that exactly one hyperbola passes through SS' . Since SS is an *ISS*, SS contains at least one point S_i that does not lie on this hyperbola. Hence, there is no hyperbola that passes through the 6 points $SS' \cup \{S_i\}$. From Theorem 1, it follows that $SS' \cup \{S_i\} \subset SS$ is an *ISS*. This contradicts the assumption that SS is an *MISS*. ■

IV. NUMBER OF INTERSECTIONS OF L_{12} AND L_{13}

Although two hyperbolas in Euclidean space may have up to 4 intersections (Corollary 3), two DTOA hyperbolas L_{12} and L_{13} may have no more than 2 intersections when S_1, S_2 , and S_3 are non-collinear. Without loss of generality (w.l.o.g), we choose our coordinate system as in Figure 4. The features of this choice are (a) $\overline{S_1S_2}$ falls on the y -axis, (b) the midpoint of $\overline{S_1S_2}$ is the origin O of the coordinate system, and (c) S_3 lies on the right side of the y -axis. We see that $\overline{S_1S_2}$, $\overline{S_2S_3}$, and $\overline{S_1S_3}$ partition the Euclidean space R^2 into seven regions (a)-(g). At most one intersection of L_{12} and L_{13} lies in the union of regions (a), (b), (f), and (g) and at most one intersection lies in

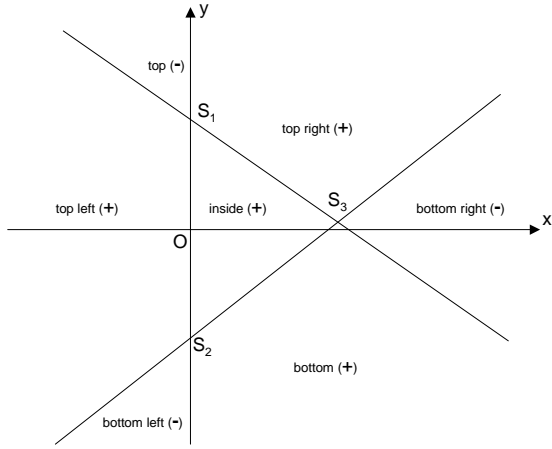


Fig. 4. Regions of monitoring area: (a) top left, (b) inside, (c) bottom right, (d) top, (e) bottom left, (f) bottom, and (g) top right. The sign of the directional derivative for each region is also given.

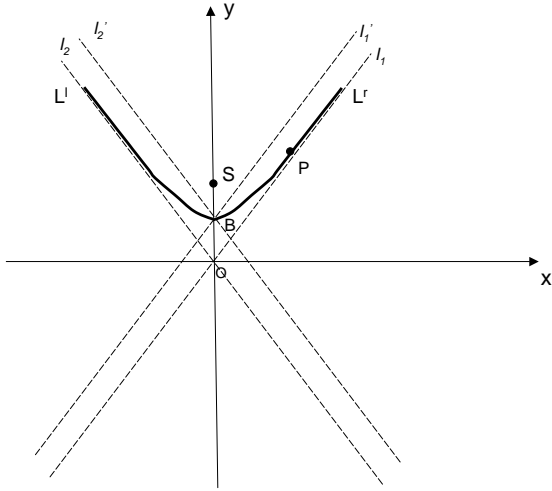


Fig. 5. A hyperbola $L = L^l \cup L^r$ with focus S and semimajor axis y -axis. The asymptotes of L are shown by two broken lines l_1 and l_2 through the origin O . The broken lines l_1' and l_2' through the vertex B are parallel to l_1 and l_2 , respectively.

the union of regions (c), (d), and (e). To prove these assertions, we need a result from [12] that establishes the monotonicity of the directional derivative of $\Delta_{13}(P)$ along the hyperbola $L_{12}(\Delta_{12}(P))$ within each of the 7 regions of Figure 4.

Theorem 5: [X. Xu, N. S. V. Rao, and S. Sahni [12]] For any point P in Euclidean space R^2 , the directional derivative of $\Delta_{13}(P)$ along the hyperbola $L_{12}(\Delta_{12}(P))$ is monotone in each of seven regions specified by three non-collinear sensors, as shown in Figure 4. The directional derivative is positive in regions (a), (b), (f), and (g), and is negative in regions (c), (d), and (e).

In the following, we use L^l and L^r to refer to the two symmetric parts (arms) of the hyperbola L (see Figure 5). The two parts L^l and L^r intersect only at the vertex B . l_1 and l_2 are the two asymptotes of the hyperbola and l_1' and l_2' are lines that intersect at the vertex B and are parallel to these asymptotes. From our choice of coordinate system, it follows that the asymptotes intersect at O .

Lemma 2: 1) $L^r(L^l)$ strictly lies between $l_1(l_2)$ and $l_1'(l_2')$.

2) The shortest Euclidean distance between a point P on L^r

(L^l) and the asymptote l_1 (l_2) decreases monotonically as P gets farther from the vertex B .

3) The shortest Euclidean distance between a point P on L^r (L^l) and the line l_1' (l_2') increases monotonically as P gets farther from the vertex B .

Proof: Follows from the definition of a hyperbola, its asymptotes, and the lines l_1' and l_2' . ■

In Theorem 6, we show that when S_1 is closer to the source S than are S_2 and S_3 , $L_{12}(\Delta_{12}(S))$ and $L_{13}(\Delta_{13}(S))$ have at most 2 intersections including the source S . This restriction on the source being closer to S_1 than the remaining two sensors is removed in Theorem 7. We often use L_{ij} as an abbreviation for $L_{ij}(\Delta_{ij}(S))$.

Theorem 6: When S_1 is closer to the source S than are S_2 and S_3 , L_{12} and L_{13} have at most 2 intersections.

Proof:

Let $P_i = (x_i, y_i)$, $1 \leq i \leq m$ be intersections of L_{12} and L_{13} . From the definition of a hyperbola, it follows that $\Delta_{12}(P_i) = \Delta_{12}(P_{i'})$ and $\Delta_{13}(P_i) = \Delta_{13}(P_{i'})$ for $1 \leq i < i' \leq m$.

There are 4 possible cases for the relationship between the line $\overline{S_2S_3}$ and the hyperbola L_{12} —(1) the line is below L_{12}^l , (2) the line intersects L_{12}^l , (3) the line intersects L_{12}^r and $\angle S_3S_1S_2 \geq 90^\circ$, and (4) the line intersects L_{12}^r and $\angle S_3S_1S_2 < 90^\circ$. These 4 cases are shown in Figures 6-9, respectively. We show below that L_{12} and L_{13} have at most 2 intersections in each of these cases.

Case 1: $\overline{S_2S_3}$ lies below L_{12}

When $\overline{S_2S_3}$ lies below L_{12} , L_{12} must lie wholly within regions (a) top left, (b) inside, (d) top, and (g) top right, (Figure 6). Δ_{13} , from Theorem 5, monotonically increases in regions (a), (b), and (g) and monotonically decreases in (d). So, if no component of L_{12} is in region (d), then Δ_{13} monotonically increases along all of L_{12} and the value of Δ_{13} for each point P on L_{12} is unique. Hence, L_{12} and L_{13} have only 1 intersection. If region (d) contains a portion of L_{12} , then when one moves the point P from left to right along L_{12} , (d) is the first region to be visited. So, when moving from left to right along L_{12} , Δ_{13} monotonically decreases while we are moving along the portion of L_{12} that is inside region (d) and then monotonically increases for the remainder of L_{12} . Hence L_{12} has at most 2 distinct points for any given value of Δ_{13} . So, L_{12} and L_{13} have at most 2 intersections.

Case 2: $\overline{S_2S_3}$ intersects L_{12}^l

When $\overline{S_2S_3}$ intersects L_{12}^l , $\angle S_3S_2S_1 > 90^\circ$ (Figure 7). So, L_{12} cannot have a component in either of the regions (c) (bottom right) and (f) (bottom). Additionally, L_{12} cannot have a component in region (d) (top). To see this, observe that L_{12}^r is wholly to the right of the y -axis while region (d) is wholly to the left of this axis. So, no portion of L_{12}^r is in region (d). To see that no portion of L_{12}^l is in region (d) either, note that L_{12}^l is below l_2' (Lemma 2). Since, $\overline{S_2S_3}$ intersects L_{12}^l and l_2 is strictly below L_{12}^l (Lemma 2), $\overline{S_2S_3}$ intersects the asymptote l_2 . Now, since l_2' is parallel to l_2 , $\overline{S_2S_3}$ also intersects l_2' , which implies that the slope of $\overline{S_2S_3}$ is less than that of l_2' . Hence, the slope of $\overline{S_1S_3}$ is less than that of l_2' . From this, the fact that L_{12}^l lies below l_2' , and the fact that the intersection (vertex B of L_{12}) of L_{12}^l and l_2' is below S_1 , it follows that no portion

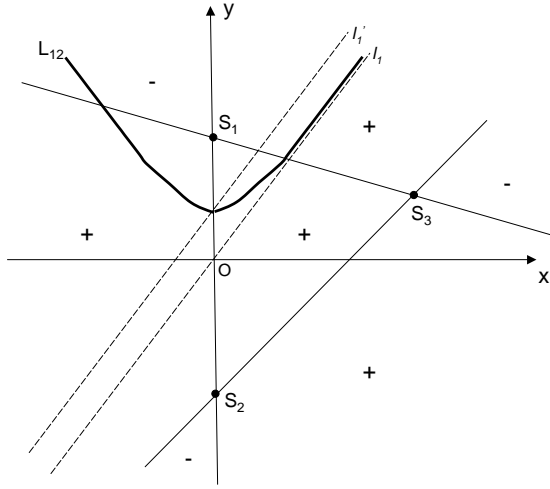


Fig. 6. Case 1: $\overline{S_2S_3}$ lies below L_{12}

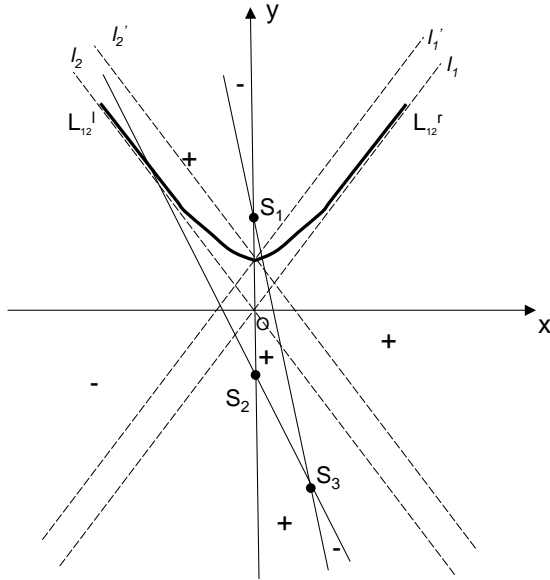


Fig. 7. Case 2: $\overline{S_2S_3}$ intersects L'_{12}

of L'_{12} is inside the top region (d).

Consequently, as one moves from left to right along L_{12} , the region (e) (i.e., bottom left) is the first region to be visited. Δ_{13} monotonically decreases inside this region and monotonically increases in the remaining regions that L_{12} is in. Hence L_{12} has at most 2 distinct points for any given value of Δ_{13} . So, L_{12} and L_{13} have at most 2 intersections.

Case 3: $\overline{S_2S_3}$ intersects L'_{12} and $\angle S_3S_1S_2 \geq 90$

In this case, region (e) (bottom left) lies entirely below L_{12} (Figure 8). Hence, no portion of L_{12} is in region (e). Since $\angle S_3S_1S_2 \geq 90$, $\theta < 90$ (see Figure 8). Hence, $d(P, S_1) > d(P, S_3)$ for every point P inside region (c) (bottom right). Since, by assumption, S_1 is closer to the source S than is S_3 , no portion of L_{13} is in region (c). Hence, L_{12} and L_{13} have no intersection in region (c).

If L_{12} has an overlap with region (d) (top), then region (d) is the first region encountered as we move from left to right along L_{12} and if L_{12} overlaps with region (c) (bottom right), region (c) is the last region encountered as we move

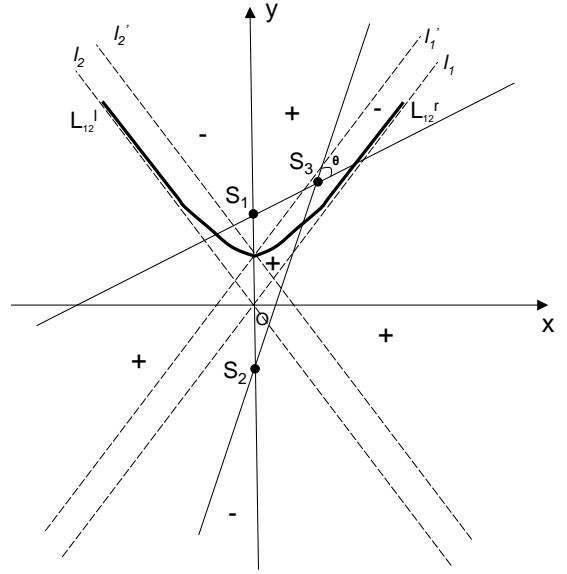


Fig. 8. Case 3: $\overline{S_2S_3}$ intersects L'_{12} and $\angle S_3S_1S_2 \geq 90$.

from left to right along L_{12} . Δ_{13} monotonically decreases in region (d), L_{12} and L_{13} do not intersect in region (c), and Δ_{13} monotonically increases in the remaining regions that L_{12} may overlap. So, L_{12} and L_{13} have at most 2 intersections.

Case 4: $\overline{S_2S_3}$ intersects L'_{12} and $\angle S_3S_1S_2 < 90$

As in Case 3, no portion of L_{12} is in region (e) (bottom left). Further, L_{13} may overlap with either region (c) (bottom right) or region (d) (top) but not both. To see this, suppose that L_{13} overlaps with region (c). For this to happen, L'_{13} must cross $\overline{S_2S_3}$. Using an argument similar to that used in Case 2, we may show that the slope of $\overline{S_2S_3}$ is greater than that of L'_{13} . Furthermore, the remaining portion of L'_{13} once after crossing $\overline{S_2S_3}$ lies strictly below $\overline{S_2S_3}$. So, no portion of L'_{13} is in region (d). Since L'_{13} is to the left of S_1S_3 , no portion of L'_{13} is in region (d) either. So, L_{13} may overlap only one of the regions (c) and (d). Therefore, L_{12} and L_{13} cannot have an intersection in both region (c) and region (d). Finally, if a portion of L_{12} is in region (d), region (d) is the first region encountered as we move along L_{12} from left to right and if a portion of L_{12} is in region (c), then region (c) is the last region encountered. Δ_{13} monotonically decreases as we move from left to right along L_{12} inside regions (c) and (d) and monotonically increases in the remaining regions that L_{12} overlaps. So, L_{12} and L_{13} have at most 2 intersections. ■

Theorem 7: L_{12} and L_{13} have at most 2 intersections.

Proof:

Since, $\Delta_{23}(P) = \Delta_{13}(P) - \Delta_{12}(P)$ for every point P , the hyperbola pairs (L_{12}, L_{13}) , (L_{12}, L_{23}) , and (L_{13}, L_{23}) have the same set of intersections. Suppose, w.l.o.g., that the source is closer to S_2 than to S_1 and S_3 . It follows from Theorem 6 that L_{21} and L_{23} have at most 2 intersections. Hence, L_{12} and L_{13} have at most 2 intersections. ■

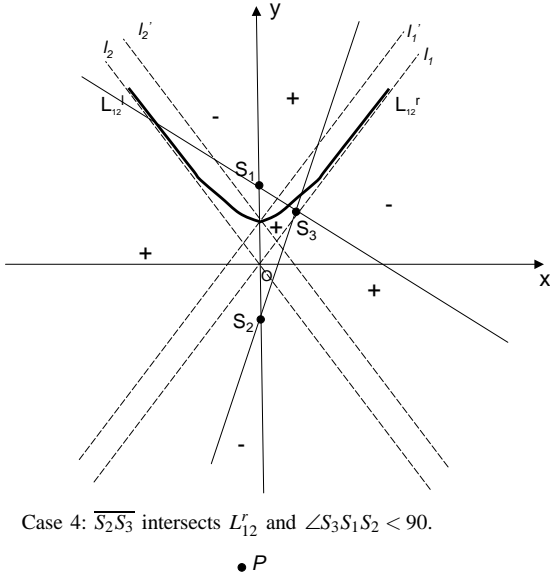


Fig. 9. Case 4: $\overline{S_2S_3}$ intersects L_{12}^r and $\angle S_3S_1S_2 < 90^\circ$.

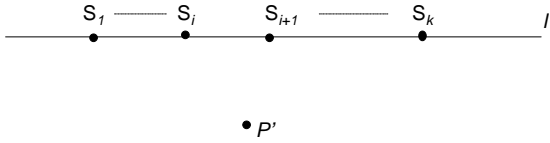


Fig. 10. Collinear sensors

V. INDISTINGUISHABLE POINTS

When SS is not an ISS , there is at least one pair of distinct points that are indistinguishable. That is, there are distinct points P_1 and P_2 for which $\Delta_{ij}(P_1) = \Delta_{ij}(P_2)$, $1 \leq i < j \leq k$ (or equivalently, $\Delta_{1j}(P_1) = \Delta_{1j}(P_2)$, $2 \leq j \leq k$). P_1 and P_2 are dual points. When SS is an ISS , no point P has a dual. In this section, we first show that the indistinguishable relation is an equivalence relation. Then, we show that each point P may have at most 1 dual point.

Theorem 8: The *indistinguishable* relation is an equivalence relation on R^2 .

Proof:

A relation is an equivalence relation iff it is reflexive, symmetric, and transitive. Reflexivity is immediate as a point is indistinguishable from itself. Also, if P_1 and P_2 are indistinguishable then so also are P_2 and P_1 . So, the relation is symmetric. For any three points P_1 , P_2 , and P_3 such that P_1 and P_2 are indistinguishable and P_2 and P_3 are indistinguishable, we have $\Delta_{ij}(P_1) = d(P_1, S_i) - d(P_1, S_j) = d(P_2, S_i) - d(P_2, S_j) = \Delta_{ij}(P_2)$ and $\Delta_{ij}(P_2) = d(P_2, S_i) - d(P_2, S_j) = d(P_3, S_i) - d(P_3, S_j) = \Delta_{ij}(P_3)$, $1 \leq i < j \leq k$. So, $\Delta_{ij}(P_1) = d(P_1, S_i) - d(P_1, S_j) = d(P_3, S_i) - d(P_3, S_j) = \Delta_{ij}(P_3)$, $1 \leq i < j \leq k$. Hence, the *indistinguishable* relation is transitive. ■

Clearly, the *indistinguishable* relation partitions Euclidean space R^2 into a collection of disjoint equivalence classes. If SS is an ISS , then each equivalence class is of unit cardinality; otherwise, the cardinality of at least one equivalence class is more than 1.

When $k = 2$, each equivalence class corresponds to a hyperbola with foci S_1 and S_2 and vice versa. The cardinality of

each equivalence class in this case is infinite. When $k > 2$ and the sensors are collinear (Figure 10), each point on the line segment $\overline{S_1S_k}$, exclusive of S_1 and S_k , defines an equivalence class of unit cardinality because no such point has a dual. All points on the line l that runs through the collinear sensors and that are to the left (right) of $S_1(S_k)$, inclusive, form an equivalence class of infinite cardinality. For each point P not on the line l , has a single dual point P' that is the reflection of P with respect to l . Point P and its dual P' define an equivalence class of cardinality 2.

When the sensors are not collinear (this can happen only when $k > 2$), Theorem 9 establishes that the cardinality of each equivalence class is at most 2.

Theorem 9: When the sensors are not collinear, the cardinality of each equivalence class defined by the indistinguishable relation is at most 2.

Proof:

We prove this by contradiction. Let SS be the sensor set. Suppose there is an equivalence class whose cardinality is more than 2. Let P_1 , P_2 , and P_3 be any three points in this equivalence class. Since P_1 and P_2 are indistinguishable, from the proof of Theorem 1, it follows that there is a hyperbola L_{12} , whose foci are P_1 and P_2 , that passes through the points of SS . Similarly, there is a hyperbola L_{13} , whose foci are P_1 and P_3 , that passes through the points of SS . L_{12} and L_{13} intersect at at least the points of SS , which are more than 2 in number. This contradicts Theorem 7, which states that these two hyperbola may have at most two intersections. ■

VI. ISSS FOR POLYGONAL REGIONS

Although 4 properly positioned sensors are required to uniquely identify a source in Euclidean space (Theorem 2), in many real-world applications, the monitoring region is bounded by a polygon and 3 sensors suffice. We assume that the sensors are restricted to be placed on or inside the bounding polygon. As an aside, we note that when the monitoring region is a simple line segment, say $\overline{S_iS_j}$, then two sensors placed at S_i and S_j , respectively, are sufficient to uniquely identify any source on this segment. To see this, observe that as we move P from S_i to S_j along the line segment $\overline{S_iS_j}$, $\Delta_{ij}(P)$ varies monotonically from $-d(S_i, S_j)$ to $d(S_i, S_j)$. Hence, there is no pair of indistinguishable points on this segment.

Lemma 3: Every non-degenerate simple polygon has an $MISS$ whose size is 3.

Proof:

Case 1: The simple polygon is convex.

Let S_1 and S_2 be the end points of an edge of the polygon. Let S_3 be any other point on this edge. Note that the 3 chosen points are collinear and the entire convex polygon lies on one side of the edge that these 3 points lie on. From the discussion preceding Theorem 9, it follows that the dual of every point of the polygon that is not on this edge is on the other side of this edge. Points on the edge either have no dual or have dual(s) outside the polygon. Hence every point in or on the polygon is uniquely identifiable and $\{S_1, S_2, S_3\}$ is a size 3 $MISS$ for the polygon.

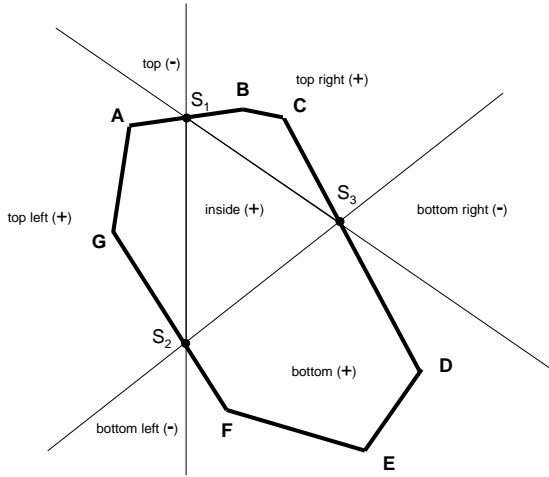


Fig. 11. Sensors S_1 , S_2 , and S_3 on the boundary of a convex polygon. The 7 planar regions induced by these 3 sensors are (a) top left, (b) inside, (c) bottom right, (d) top, (e) bottom left, (f) bottom, and (g) top right. The sign of the directional derivative for each region is also shown.

An alternative construction for a size 3 *MISS* is to consider any 3 non-collinear points S_1 , S_2 , and S_3 that are on the boundary of the polygon (Figure 11). Now, the entire convex polygon must be contained in the union of four regions: (a) top left, (b) inside, (f) bottom, and (g) top right. From Theorem 5, the directional derivative of Δ_{13} along L_{12} increases monotonically in each of these four regions. Further, the intersection of L_{12} and the convex polygon is a continuous curve C that is limited to these four regions (see Theorem 6). Since, Δ_{13} is monotonically increasing along C , L_{12} and L_{13} have at most one intersection on C . Hence, every point in or on the convex polygon is uniquely identifiable.

Case 2: The simple polygon is concave.

We start with a minimum bounding convex polygon of the concave polygon (Figure 12). Let S_1 , S_2 , and S_3 be any three points on the intersection of the boundary of these concave and convex polygons. From Case 1, it follows that every point in and on the boundary of the convex bounding polygon, and so every point in and on the boundary of the concave polygon, is uniquely identifiable.

In Lemma 3, we prove that by choosing 3 sensor locations on the boundary of a simple polygon, an *SS* of size 3 uniquely identifies any source S on or inside a simple polygon. We show in Lemma 4 when a sensor is placed strictly inside a simple polygon, 3 sensors are not sufficient to uniquely identify every point in or on the polygon.

Lemma 4: Let *SS* be an *ISS* set for a non-degenerate simple polygon. If at least one location of *SS* is inside the polygon, $|SS| \geq 4$.

Proof:

Suppose that *SS* is an *ISS* and that $|SS| = 3$. W.l.o.g, assume S_1 lies inside the simple polygon as shown in Figure 13. Note that a portion of the simple polygon must lie inside the top region. We may choose two negative constants δ_{12} and δ_{13} , such that $L_{12}(\delta_{12})$ and $L_{13}(\delta_{13})$ intersect at two distinct points P_1 in the top region and P_2 in the top left region. Since both

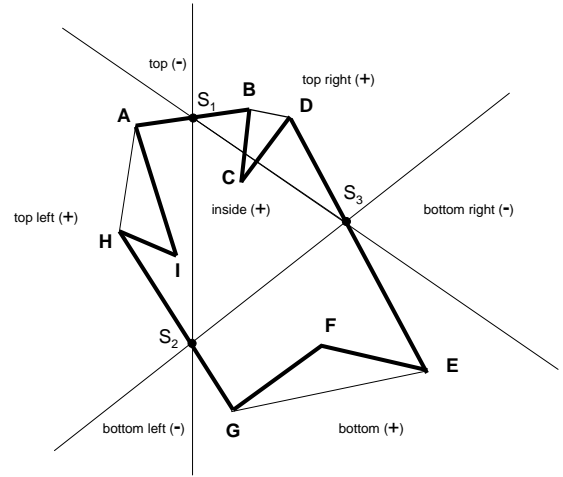


Fig. 12. A concave polygon, its bounding convex polygon, and three sensors S_1 , S_2 , and S_3 placed on the common boundary of the concave and convex polygons

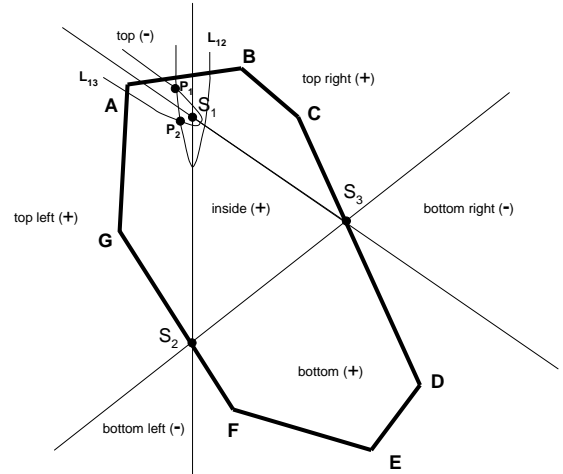


Fig. 13. S_1 lies inside a simple polygon while S_2 and S_3 are on the boundary. P_1 in the top region is a dual point of P_2 which lies in the top left region.

P_1 and P_2 are inside the simple polygon and P_1 is the dual of P_2 , *SS* is not an *ISS* for the points of the simple polygon. ■

Theorem 10: 3 sensors can uniquely identify any source in or on a non-degenerate simple polygon iff the sensors are on the common boundary of the given polygon and its minimum bounding convex polygon. In case the 3 boundary sensors are collinear, 2 must be at the end points of an edge of the bounding convex polygon and the third at an in-between point.

Proof:

Follows from Lemmas 3 and 4. ■

VII. CONCLUSIONS

In this paper, we studied the impact of sensor deployment on the uniqueness of source estimate in Euclidean plane as well as in a simple polygon. We derived necessary and sufficient conditions for each case. A tight bound on the size of a minimal identifying sensor set in R^2 was given. We re-investigated the number of intersections of two hyperbolas having a common focus, and showed it to be at most 2. Specifically, at most one intersection lies in the union of

inside region, top left region, top right region, and bottom region, while at most one intersection lies in the union of top region, bottom left region, and bottom right region. Each sensor deployment corresponds to an equivalence relation on R^2 . For each identifying sensor set, each equivalence class is of unit cardinality. For each non-identifying sensor set, at least one equivalence class is of greater than unit cardinality.

There are several future directions to be considered. It would be interesting to study the effect of randomness in distance-differences, which could be due to measurement errors or due to the underlying process. In particular, it would be interesting to investigate the effects on both uniqueness and minimality results presented in this paper. Applications of these methods to practical radiation detection systems would be of future interest.

ACKNOWLEDGMENTS

This work is funded by the SensorNet program at Oak Ridge National Laboratory (ORNL) through Office of Naval Research. ORNL is managed by UT-Battelle, LLC for U.S. Department of Energy under Contract No. DE-AC05-00OR22725.

REFERENCES

- [1] R. Schmidt, "A new approach to geometry of range difference location," *IEEE Trans. on Aerospace and Electronic Systems*, vol. 8, no. 3, 1972.
- [2] G. Mellen, M. Pachter, and J. Raquet, "Closed-form solution for determining emitter location using time difference of arrival measurements," *IEEE Trans. on Aerospace and Electronic Systems*, vol. 39, no. 3, pp. 1056–1058, 2003.
- [3] A. H. Sayed, A. Tarighat, and N. Khajehnouri, Network-based wireless location, *IEEE Signal Processing Magazine*, pp. 24–40, July 2005.
- [4] F. Zhao and L. Guibas, *Wireless Sensor Networks*, Elsevier, 2004.
- [5] B. Krishnamachari, Ed., *Networking Wireless Sensors*, Cambridge University Press, 2005.
- [6] H. C. Schau and A. Z. Robinson, "Passive source localization employing intersecting spherical surfaces from time-of-arrival differences," *IEEE Trans. on Acoustics, Speech, and Signal Processing*, vol. 35, no. 8, pp. 1223–1225, 1987.
- [7] Y. T. Chan and K. C. Ho, "A simple and efficient estimator for hyperbolic location," *IEEE Trans. on Image Processing*, vol. 42, no. 8, pp. 1905–1915, 1994.
- [8] B. T. Fang, "Simple solutions for hyperbolic and related position fixes," *IEEE Transactions on Systems, Man and Cybernetics-B*, vol. 26, no. 9, pp. 748–753, 2005.
- [9] F. Gustafsson and F. Gunnarson, Positioning using time-difference of arrival measurements, *IEEE International Conference on Acoustics, Speech, and Signal Processing (ICASSP'03)*, 2003.
- [10] N. S. V. Rao, "Identification of simple product-form plumes using networks of sensors with random errors," in *International Conference on Information Fusion*, 2006.
- [11] N. S. V. Rao, X. Xu, and S. Sahni, "A Computational Geometry Method for DTOA Triangulation," submitted to *International Conference on Information Fusion*, 2007.
- [12] X. Xu, N. S. V. Rao, and S. Sahni, "A computational geometric method for triangulation using differences of distances," *ACM Transactions on Sensor Networks*, to appear.
- [13] F. Kirwan, "Complex Algebraic Curves," United Kingdom: Cambridge University Press, 1992.